Physics of the Earth and Planetary Interiors, 65 (1990) 15–27
Elsevier Science Publishers B.V., Amsterdam

Micromagnetic formulation for the personal computer

V.P. Shcherbakov [1], P.W. Schmidt [2], N.K. Sycheva [3] and B.E. Lamash [1]

[1] *Borok Geophysical Observatory, Institute of Physics of the Earth, U.S.S.R. Academy of Sciences, Moscow 123242 (U.S.S.R.)*
[2] *CSIRO Division of Exploration Geoscience, P.O. Box 136, North Ryde, NSW, 2113 (Australia)*
[3] *Physical and Technical Institute, Far East State University, Suhanova 8, Vladivostok 690600 (U.S.S.R.)*

(Received November 30, 1989; revision accepted April 9, 1990)

ABSTRACT

Shcherbakov, V.P., Schmidt, P.W., Sycheva, N.K. and Lamash, B.E., 1990. Micromagnetic formulation for the personal computer. Phys. Earth Planet. Inter., 65: 15–27.

Algorithms for calculating the equilibrium energy state of a three-dimensional ferromagnetic particle according to an earlier micromagnetic formulation can now be implemented on a personal computer (PC). Some PC enhancement boards are now very fast by normal standards. For instance, the Mercury 6400 is rated at 20 MFlops (million floating point operations per second). The 20-MHz Definicon DSIT4-1/800 transputer, used for much of the present work, although slower (1.5 MFlops), is still able to perform the numerical convergence in a respectable time by using a progressive minimization procedure. Other numerical techniques which have employed supercomputers arrive at similar estimations of energy levels and magnetic structure; this indicates that the present technique is dependable. Several examples that demonstrate this are discussed.

1. Introduction

The study of micromagnetic structures is important in rock magnetism and palaeomagnetism because theory predicts a quantum jump between the magnetic properties of single-domain (SD) and multi-domain (MD) particles, whereas experimentally there is a smooth continuous change from one regime to the other (see Dunlop, 1977). An examination of recent work in this field (Moskowitz and Banerjee, 1979; Moon and Merrill, 1984; Enkin and Dunlop, 1987; Williams and Dunlop, 1989) reveals a consensus of opinion that the critical size for transformation from uniform SD structure to non-uniform structure is $\sim 0.1\ \mu$m for magnetite. For grain sizes above this threshold there may be two or more stable structures. In larger grains, such as those that have been observed with Bitter pattern techniques (Halgedahl and Fuller, 1983), closure domains or surface spin structure (Williams and Dunlop, 1989) arise to reduce flux leakage and may disguise the internal structure.

2. Description of model

The micromagnetic approximation of the free energy density of a ferromagnetic material is well known and can be written as the sum of the exchange energy density (E_E), the magnetocrystalline energy density (E_A), the magnetoelastic energy density (E_S), the magnetostatic self-energy density (E_D) and the external field energy density (E_H). Omitting the magnetoelastic energy (for reasons explained below) the remaining energy densities may be expressed as

$$E_E = A_{ex}\left[(\nabla A)^2 + (\nabla B)^2 + (\nabla C)^2\right] \quad (1)$$

where A_{ex} is the exchange constant, and A, B and C are direction cosines of the spontaneous magnetization vector, $\mathbf{I}_s$,

$$E_A = K(A^2B^2 + A^2C^2 + B^2C^2) \quad (2)$$

where K is the anisotropy constant,

$$E_D = (\mu_0/4\pi)\sum_{ij}\left[\frac{m_i m_j}{r_{ij}^3} - \frac{3(m_i r_{ij})(m_j r_{ij})}{r_{ij}^5}\right] \quad (3)$$

being the sum of the dipole–dipole interaction of atoms, where m_i and m_j are magnetic moments and r_{ij} is the distance between the ith and jth atom. It should be noted that for a finite uniformly magnetized cubic lattice the self-magnetostatic energy is zero because the double sum in eqn. (3) vanishes by symmetry. Equivalentally, this result can be interpreted as arising from the mutual cancellation of the demagnetization field and the Lorentz field (Brown, 1962, pp. 39–42). The external field energy is

$$E_H = -\mathbf{H} \cdot \mathbf{I}_s \tag{4}$$

Our approximation assumes a cube-shaped particle of side L, subdivided into N^3 cells, each cell being a cube of side L/N. Let the integers (i, j, k) represent the co-ordinates of such cell in three orthogonal axes. $A(i, j, k)$, $B(i, j, k)$ and $C(i, j, k)$ are the direction cosines of spontaneous magnetization for the ijkth cell, and $\nabla A(i, j, k)$, $\nabla B(i, j, k)$ and $\nabla C(i, j, k)$ are the derivatives of A, B and C at the ijkth cell. By the finite-difference method we may obtain

$$\begin{aligned}
&[\nabla A(i, j, k)]^2 \\
&\quad \approx \tfrac{1}{2}(N/L)^2\{[A(i, j, k) - A(i-1, j, k)]^2 \\
&\qquad + [A(i+1, j, k) - A(i, j, k)]^2 \\
&\qquad + [A(i, j, k) - A(i, j-1, k)]^2 \\
&\qquad + [A(i, j+1, k) - A(i, j, k)]^2 \\
&\qquad + [A(i, j, k+1) - A(i, j, k)]^2\} \\
&\qquad + [A(i, j, k) - A(i, j, k-1)]^2
\end{aligned} \tag{5}$$

and similar expressions for $[\nabla B(i, j, k)]^2$ and $[\nabla C(i, j, k)]^2$. We note also that it is necessary to consider the boundary conditions $(\nabla A \cdot n) = 0$, where n is a unit vector normal to the surface of the particle (the same boundary conditions apply for $\nabla \cdot B$ and $\nabla \cdot C$). In finite difference notation these boundary conditions may be expressed, in practice, as

$$\begin{aligned}
&A(i, j, k) - A(i-1, j, k) = 0 \\
&\quad \text{at } i = 1,\ i = N+1 \\
&B(i, j, k) - B(i, j-1, k) = 0 \\
&\quad \text{at } j = 1,\ j = N+1 \\
&C(i, j, k) - C(i, j, k-1) = 0 \\
&\quad \text{at } k = 1,\ k = N+1
\end{aligned} \tag{6}$$

It should be noted that the boundary conditions expressed in (6) should be considered only in the context of computation, as $A(0, j, k)$, $A(N+1, j, k)$, etc., have no physical meaning. Thus eqns. (6) are used as a set, and only for calculating the exchange energy.

Therefore the exchange energy for the ijkth cell is

$$\begin{aligned}
E_E(i, j, k) = A_{ex}(L/N)^3\big[&(\nabla A(i, j, k)^2 \\
&+ \nabla B(i, j, k)^2 + \nabla C(i, j, k)^2\big]
\end{aligned} \tag{7}$$

Analogously, the magnetocrystalline energy is

$$\begin{aligned}
&E_A(i, j, k) \\
&\quad = K(L/N)^3[A^2(i, j, k) \cdot B^2(i, j, k) \\
&\qquad + A^2(i, j, k) \cdot C^2(i, j, k) \\
&\qquad + B^2(i, j, k) \cdot C^2(i, j, k)]
\end{aligned} \tag{8}$$

For the calculation of the magnetostatic energy, E_D, we used an approximation where each cell is regarded as a dipole of moment $I_s(L/N)^3$. Then,

$$\begin{aligned}
&E_D(i, j, k) \\
&\quad = I_s^2(L/N)^3 \cdot \sum_{q=1}^{N} \sum_{m=1}^{N} \sum_{r=1}^{N} \\
&\qquad \times \Big\{\Big[\big((i-q)^2 + (j-m)^2 + (k-r)^2\big)^{1/2}\Big]^{-3} \\
&\qquad \times [A(i, j, k) \cdot A(q, m, r) \\
&\qquad + B(i, j, k) \cdot B(q, m, r) \\
&\qquad + C(i, j, k) \cdot C(q, m, r)] \\
&\qquad - 3\big[\sqrt{\,[(i-q)^2 + (j-m)^2 + (k-r)^2]\,}\big]^{-5} \\
&\qquad \times [(i-q)A(i, j, k) + (j-m)B(i, j, k) \\
&\qquad + (k-r)C(i, j, k)] \\
&\qquad \times [(i-q)A(q, m, r) \\
&\qquad + (j-m)B(q, m, r) \\
&\qquad + (k-r)C(q, m, r)]\Big\} \\
&\qquad (q, m, r) \neq (i, j, k)
\end{aligned} \tag{9}$$

If there are external factors, such as homogeneous stress, σ, or a magnetic field, **H**, then these also need to be included in the energy terms,

$$E_S(i, j, k) = 3/2\lambda\sigma \cdot A^2(i, j, k) \tag{10}$$

where λ and σ are the magnetostrictive constant and the stress, respectively, and

$$E_H(i, j, k) = -H \cdot A(i, j, k) \tag{11}$$

For simplicity, we take the magnetocrystalline easy axis, the easy axis due to stress, and the **H** direction, as the x-axis. Isotropic magnetostriction was also adopted; this requires only one magnetostrictive constant, λ.

The total energy of the particle is therefore given by

$$E_T = \sum_{q=1}^{N} \sum_{m=1}^{N} \sum_{r=1}^{N} \left(E_E + E_A + \tfrac{1}{2}E_D + E_H + E_S\right) \tag{12}$$

The factor of one-half in (12) is required because each cell is counted twice in sums (9) and (12). Our task is to find the equilibrium distribution of magnetization, or, in other words, we have to determine $3N^3$ variables, $A(i, j, k)$, $B(i, j, k)$ and $C(i, j, k)$ for $i, j, k = 1, \ldots, N$, that minimize E_T. As $A^2 + B^2 + C^2 = 1$, there are actually $2N^3$ independent variables. However, even for $N = 10$ there are 2000 variables, and normal PC minimization methods are very slow. We propose another minimization method taken from a rather simple physical principle.

Using spherical coordinates we define $\theta(i, j, k)$ and $\phi(i, j, k)$ as

$$\left.\begin{aligned} A &= \cos\theta \cdot \cos\phi \quad -\pi/2 \le \theta \le \pi/2 \\ B &= \cos\theta \cdot \sin\phi \\ C &= \sin\theta \quad -\pi \le \phi \le \pi \end{aligned}\right\} \tag{13}$$

The variables $\theta(i, j, k)$ and $\phi(i, j, k)$ are polar and azimuthal angles in some arbitrary initial state, and E° is the energy of this state. We can try to find an equilibrium for every cell (i, j, k) separately, by minimizing the total energy E_T, for θ and ϕ. For this, it is sufficient to minimize

$$\begin{aligned} \Delta E_T(i, j, k) = {} & 2E_E(i, j, k) + E_A(i, j, k) \\ & + E_D(i, j, k) + E_S(i, j, k) \\ & + E_H(i, j, k) \end{aligned} \tag{14}$$

The factor of two in the E_E term takes into account the fact that any variation in the values of θ and ϕ implies a change in the direction of spins of neighbouring cells, as spin is assumed to vary linearly between the cell centres. After computing the equilibrium $\theta'(i, j, k)$, $\phi'(i, j, k)$ for each (i, j, k), a new state for $\mathbf{I}_s(i, j, k)$ is found and a new energy, E', can be calculated. If $E' < E^\circ$, the process is repeated with E° updated to E', otherwise, it terminates and the final distribution can be considered to be an equilibrium distribution of minimum energy. The advantage of this method is that each step requires the minimization of only two variables, which may be achieved by any ordinary method. One drawback, however, is that there is no rigorous proof that the final state is an energy minimum (either absolute or metastable). However, the results reveal reasonable domain structures, so we believe that these are representative states which are very close to true energy minima.

Several comments on magnetostrictive energy are appropriate. Considering only magnetite particles, the term E_S is one to two orders of magnitude smaller than E_A or E_D. Therefore, ignoring contributions to E_T from E_S is justifiable. Moreover, calculating E_S would require the determination of the strain tensor, which consists of six independent coefficients for each cell. This, in turn, would require the minimization of eight variables for each cell. For titanomagnetite such intricacy may be necessary, but for magnetite the inclusion of magnetostriction would lead to an enormous increase in computation time, with no discernible difference in the equilibrium distribution.

3. Results

The $\mathbf{I}_s$ distributions for magnetite particles have been determined for sizes 0.02 to 0.4 μm, with

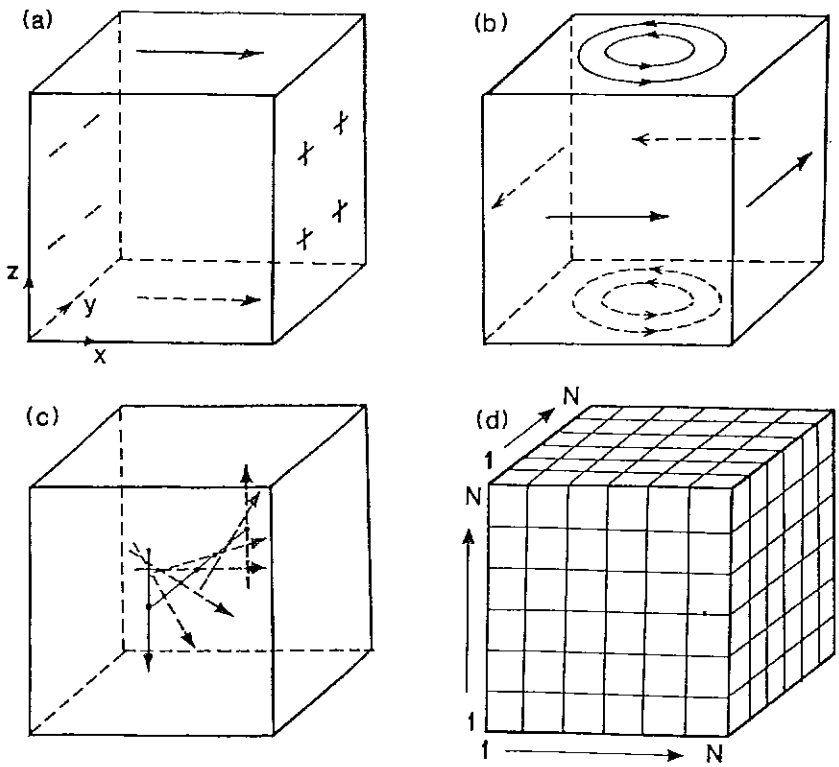

Fig. 1. Three different types of symmetry: (a) single-domain (SD), (b) curl, and (c) two-domain. The fourth cube, (d) depicts the numbering system.

values for the exchange constant, $A_{ex} = 0.67 \times 10^{11}$ J m^{-1}, the anisotropy constant, $K = -1.3 \times 10^4$ J m^{-3} and magnetite saturation magnetization, $I_s = 4.8 \times 10^5$ A m^{-1} (Moskowitz and Banerjee, 1978). Although recent values for A_{ex} are somewhat increased over the above value, simple dimensionality considerations show that grain size is proportional to $\sqrt{A_{ex}}$ so our critical sizes are slightly diminished compared with estimates using a larger value for A_{ex}.

As depicted in Fig. 1, three initial states were tested:

$$\left.\begin{aligned}
&\text{(a) 'single-domain':} && \theta = 0,\ \phi = 0\\
&\text{(b) 'two-domain':} && \theta = \pi/N\left[\tfrac{1}{2}(N+1) - j\right]\\
& && \phi = 0\\
&\text{(c) 'curling':} && \theta = 0\\
& && \phi = \tan^{-1}\left\{\frac{\left[\tfrac{1}{2}(N+1) - j\right]}{\left[\tfrac{1}{2}(N+1) - i\right]}\right\} + \pi/2;\quad i \le N/2\\
& && \phi = \tan^{-1}\left\{\frac{\left[\tfrac{1}{2}(N+1) - j\right]}{\left[\tfrac{1}{2}(N+1) - i\right]}\right\} - \pi/2;\quad i > N/2
\end{aligned}\right\} \qquad (15)$$

To reduce the computing time, we can consider only symmetrical cases where the distribution of $\mathbf{I}_s$ in different octants of the cube is symmetrical (or anti-symmetrical) with respect to some reference octant (Williams and Dunlop, 1989). The results are presented in Fig. 2 as plots of reduced net moment and reduced energy vs. grain size. The reduced net moment is obtained by dividing the net moment by $I_s l^3$, and the reduced energy is obtained by dividing the total energy, E_T, by $I_s^2 L^3$. It is useful also to mention that for truly 5D

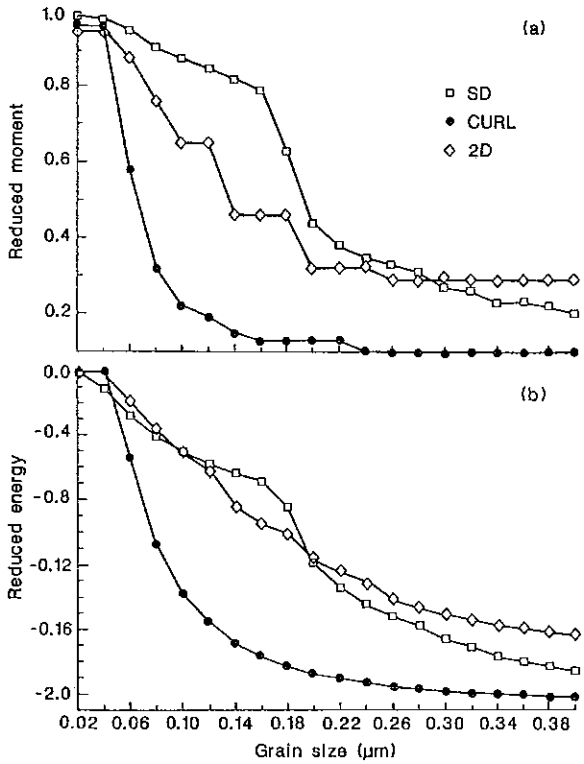

Fig. 2. Plots of (a) reduced moment and (b) reduced energy vs. grain size for calculations with imposed symmetry.

grains with a homogeneous distribution of $\mathbf{I}_s$, $E_T = 0$ if there is no external stress or magnetic field. This arises because all the energy terms in eqn. (11) are zero. Although this is obvious for the exchange and anisotropy energies, for E_D the reason is more subtle. The rigorous calculation of E_D includes the effects of both the self-demagnetizing field and the Lorentz field ($H_L = 4\pi I_s/3$), which mutually cancel each other in the case of a cube (as mentioned above).

The contribution of the Lorentz local field to the magnetostatic energy is independent of the direction of magnetisation and is usually dropped, leading to the familiar expression $E_D = \frac{1}{2}N_d I_s^2$ (Brown, 1962, pp. 101–102). The micromagnetic calculation of Williams and Dunlop (1989) did not incorporate the Lorentz field explicitly, but instead used the formulation of Rhodes and Rowland (1954). In addition, their energy was normalized by a factor $\frac{1}{2}(4\pi/3)I_s^2L^3$ so that their reduced energy

$$E_{WD} = \left[E_{SSSL}I_s^2L^3 + \tfrac{1}{2}(4\pi/3)I_s^2L^3\right] / \left[\left(\tfrac{1}{2}4\pi/3\right)I_s^2L^3\right] \quad (16)$$

where the subscripts refer to the initials of Williams and Dunlop, and of the present authors. The second term in the numerator refers to the Lorentz field energy. It is simple to derive the relationship between the reduced energy we calculate, $E/I_s^2L^3$, and the energy Williams and Dunlop (1989) calculated:

$$E_{SSSL} = (2\pi/3)(E_{WD} - 1) \quad (17)$$

For all cases, the results have been derived by beginning with a particle size of 0.02 μm, determining the equilibrium structure, increasing the grain size by 0.02 μm and repeating the calculation, and so forth. When SD structure (Fig. 1a) was imposed, an essentially SD-like structure persisted until 0.2 μm (Fig. 2a). At the other extreme, when curling structure (Fig. 1b) was imposed, the SD structure determined initially quickly collapses at 0.06 μm. For two-domain structure, the moment decays in an intermediate fashion, with a number of steps suggesting some local energy minima (LEM). The curling mode reaches a minimum (reduced) moment of 0.1 at 0.24 μm, whereas for the two-domain mode, representing the other extreme for the larger sizes, a stable (reduced) moment is reached at just under 0.3.

Appendix 1 shows the configurations of vector arrays for each situation, at 0.04 μm and for sizes for which an appreciable change in moment and energy has occurred. As we are dealing with three-dimensional (3D) structure, at least two two-dimensional (2D) projections are necessary to visualize the configurations. In all cases, the viewing axes we have chosen are the x-axis and the z-axis. These are plotted side by side for each case. Appendix 1.1 shows the transformation of an SD structure (0.04 μm) into a five-domain structure analogous to 'type 1B' of Williams and Dunlop (1989). As a reassurance that different workers are arriving at essentially identical results by different means, we note that the reduced energy calculated for a 0.1-μm particle following the method outlined by Williams and Dunlop (1989), but using the same exchange constant used here, is -0.501 (W. Williams, personal communication, 1989) compared with our value of -0.503.

The other vector arrays in Appendix 1 show the transformation of SD structure into a curl structure in curl mode (Appendix 1.2), and into a

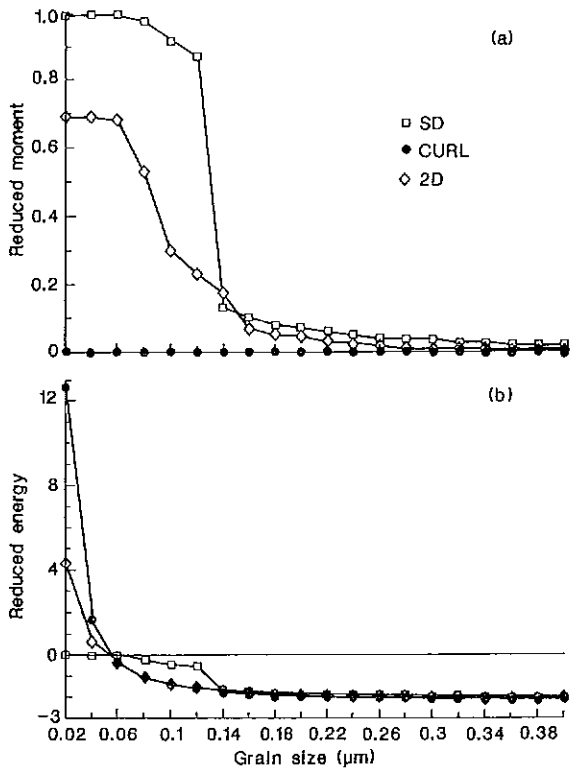

Fig. 3. Plots of (a) reduced moment and (b) reduced energy vs. grain size for calculations with no imposed symmetry, i.e. unconstrained. It should be noted that the moment of the curl state is everywhere zero.

multi-domain structure in two-domain mode (Appendix 1.3). This latter structure may be compared with that found in SD mode, also for 0.2 μm. Figure 2 shows that these configurations have almost the same energy, although the 'two-domain' moment is considerably less. The multi-domain structure is not dissimilar to the type 1B structure of Williams and Dunlop (1989) in the body of the grain, but is almost opposite on the surface. Overall though, the curl mode has a considerably lower energy (and moment) for grain sizes 0.06 μm and above, and would appear to be the most desired state. This seems to be similar to the type 2 of Williams and Dunlop (1989), who described this structure of low-energy state as two-domain with large closure domains.

As well as for cases with imposed symmetry, we have also considered more general unconstrained cases. In Fig. 3, it can be seen that, for $L > 0.14$ μm, irrespective of the initial configuration, the reduced moments and energies are very similar. Appendix 2 displays the various transformations. Whorl-like asymmetrical structures, with reduced moments of much less than 0.1, develop from the SD (Appendix 2.1) and two-domain (Appendix 2.3) initial structures, whereas the curl structure remains symmetrical (Appendix 2.2). In fact, the moment for this structure remains zero even for the smallest sizes (0.02 and 0.04 μm), although the reduced energies for these cases are large, reflecting their improbability of being realistic structures for these sizes. For small grains the curl structure is apparently stable to our unconstrained cell-by-cell minimization procedure. Using our minimization method, instability of the curl structure develops only when symmetry is imposed. Thus for the small grain sizes the unconstrained solution is erroneous. This is true also for the 0.02- and 0.04-μm sizes of the two-domain initial configuration. However, for sizes 0.08–0.14 μm, the curl and two-domain cases are energetically favoured over the SD case.

4. Conclusions

Our main conclusion is that different groups working on the micromagnetic problem are arriving at similar results using different methods, and making different assumptions. This is reassuring. In unconstrained cases, the starting configurations converge to structures that differ in detail, although their energies are essentially identical for grain sizes above 0.14 μm. This suggests that for relatively large (yet sub-micron) sized magnetite particles, there exist not only several metastable states, as proposed by Moon and Merrill (1988), but a large set of such states, with very small differences in energy. Perhaps in the limit, as $L \rightarrow \infty$, a continuum of metastable states can exist.

If a continuum of metastable states is real for larger submicron magnetite grains, such a system behaves non-ergodically and cannot be described by simple thermodynamics, but is discussed more appropriately in terms of 'spin-glasses'. For this reason the blocking temperature, T_b, could be related to the freezing temperature. Also, as magnetic viscosity is an essential property of a non-

ergodic system, the acquisition of viscous remanence does not require any special cause—diffusion of impurities or vacancies, or lattice defects, stresses, and so forth—although all these can help to enhance the viscosity.

Acknowledgements

This collaborative work was funded by the U.S.S.R. Academy of Science, CSIRO and the Australian/U.S.S.R. Science and Technology Agreement. David Clark is thanked for many discussions and suggestions to clarify some sections. The anonymous reviewers are thanked for their suggestions on improvements to the manuscript.

References

Brown, Jr., W.F., 1962. Magnetostatic Principles of Ferromagnetism. North-Holland, Amsterdam.

Dunlop, D.J., 1977. The hunting of the 'Psark'. J. Geomagn. Geoelectr., 29: 293–318.

Enkin, R.J. and Dunlop, D.J., 1987. A micromagnetic study of pseudo-single-domain remanence in magnetite. J. Geophys. Res., 92: 12 726–12 740.

Halgedahl, S. and Fuller, M., 1983. The dependence of magnetic domain structure upon magnetization state with emphasis upon nucleation as a mechanism for pseudo-single-domain behavior. J. Geophys. Res., 88: 6505–6522.

Moon, T.S. and Merrill, R.T., 1984. The magnetic moment of nonuniformly magnetized grains. Phys. Earth Planet. Inter., 34: 186–194.

Moskowitz, B.M. and Banerjee, S.K., 1979. Grain size limits for pseudo-single-domain behavior in magnetite: implications for paleomagnetism. IEEE Trans., MAG15: 1241–1246.

Rhodes, P. and Rowland, G., 1954. Demagnetizing energies of uniformly magnetized rectangular blocks. Proc. Leeds Philos. Lit. Soc., Sci. Sect., 6: 191–210.

Williams, W. and Dunlop, D.J., 1989. Three-dimensional micromagnetic modelling of ferromagnetic domain structure. Nature 337: 634–637.

Appendix 1.1.

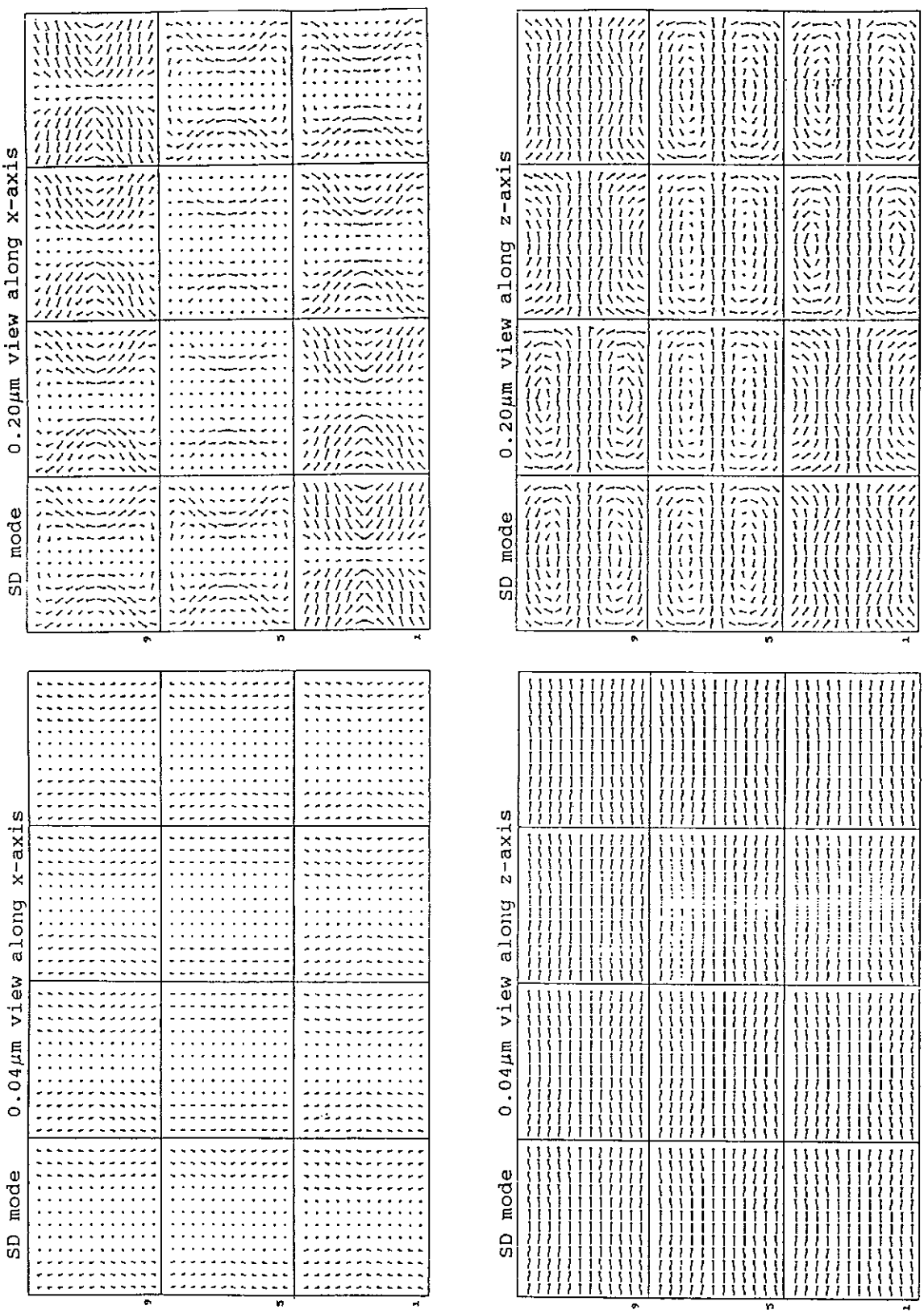
SD mode
0.04μm view along x-axis
0.20μm view along x-axis
0.04μm view along z-axis
0.20μm view along z-axis
9
5
1

Appendix 1.2.

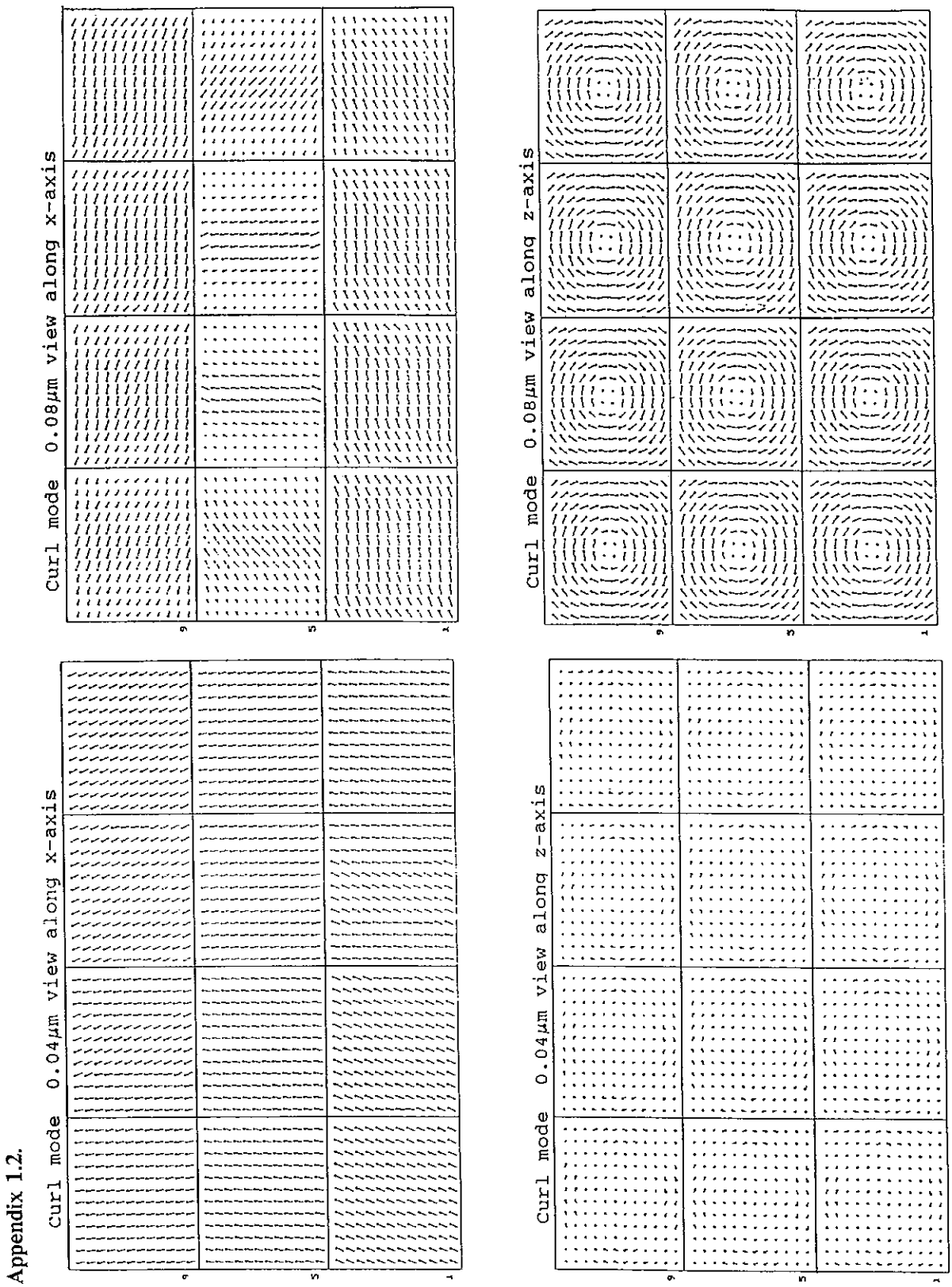
Curl mode 0.04μm view along x-axis
Curl mode 0.08μm view along x-axis
Curl mode 0.04μm view along z-axis
Curl mode 0.08μm view along z-axis

Appendix 1.3.

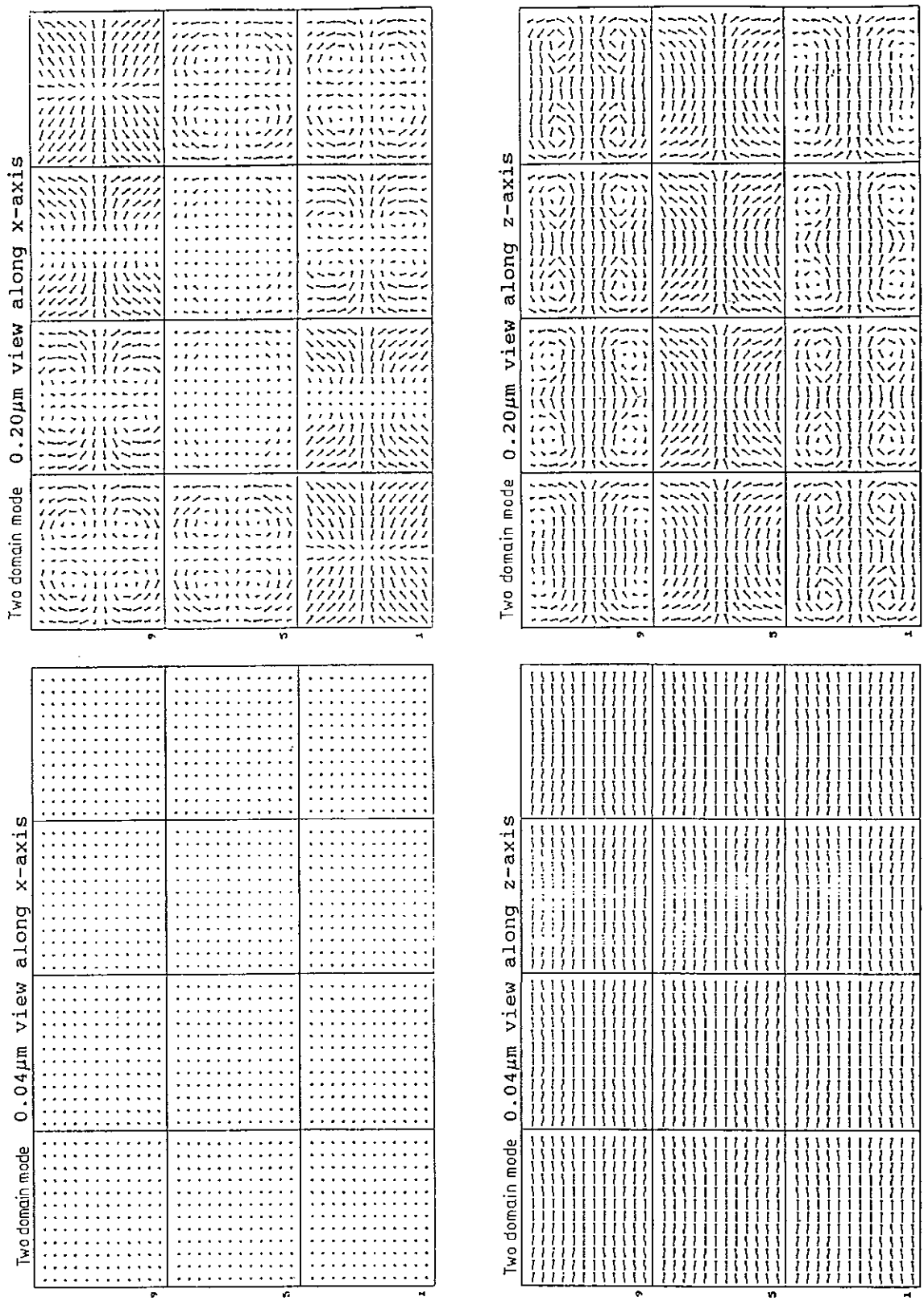
Two domain mode 0.04μm view along x-axis
Two domain mode 0.20μm view along x-axis
Two domain mode 0.04μm view along z-axis
Two domain mode 0.20μm view along z-axis

Appendix 2.1.

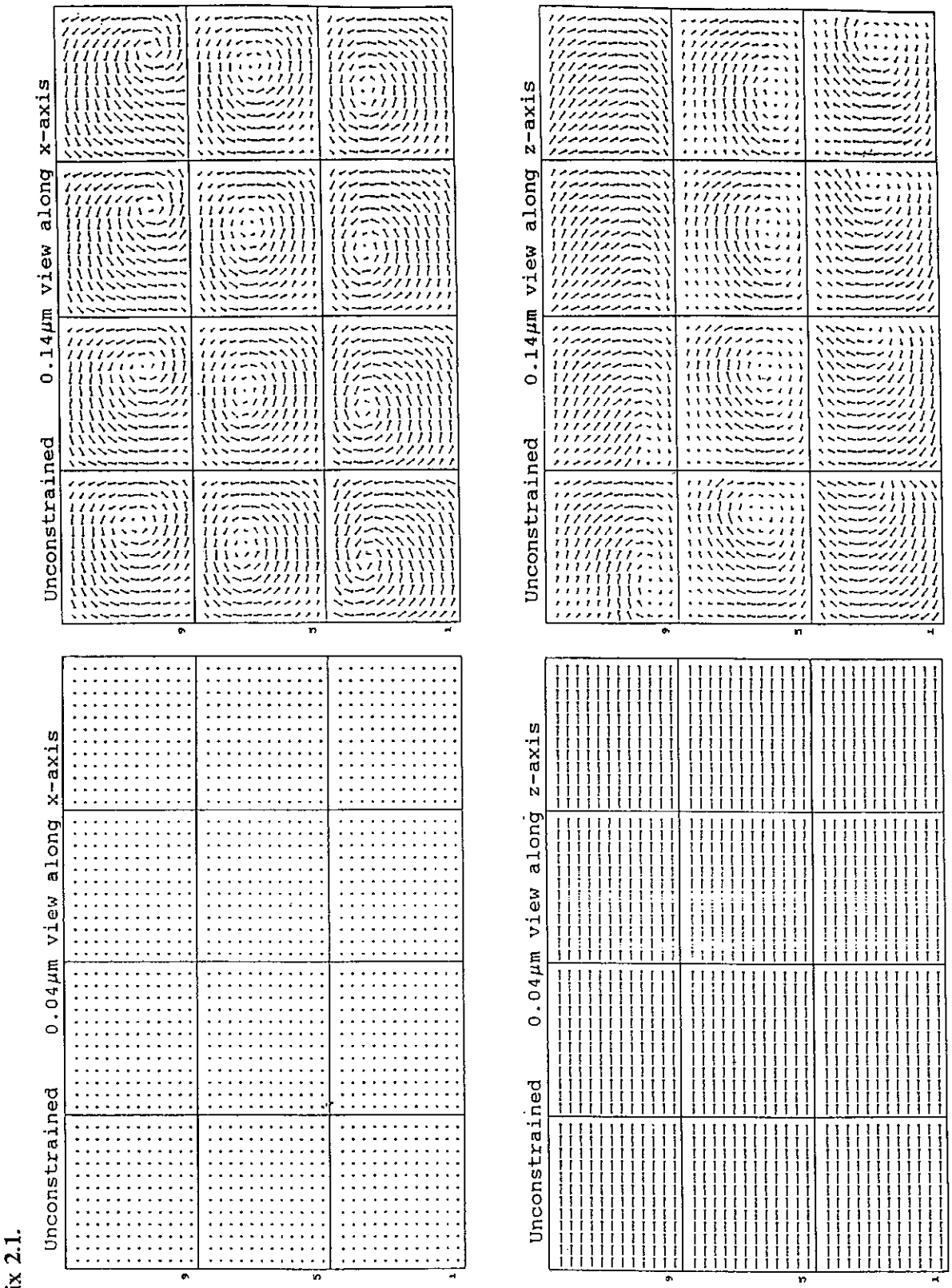
Initial state
SD
Unconstrained 0.04μm view along x-axis
Unconstrained 0.14μm view along x-axis
Unconstrained 0.04μm view along z-axis
Unconstrained 0.14μm view along z-axis

Appendix 2.2.

Initial state

Curl

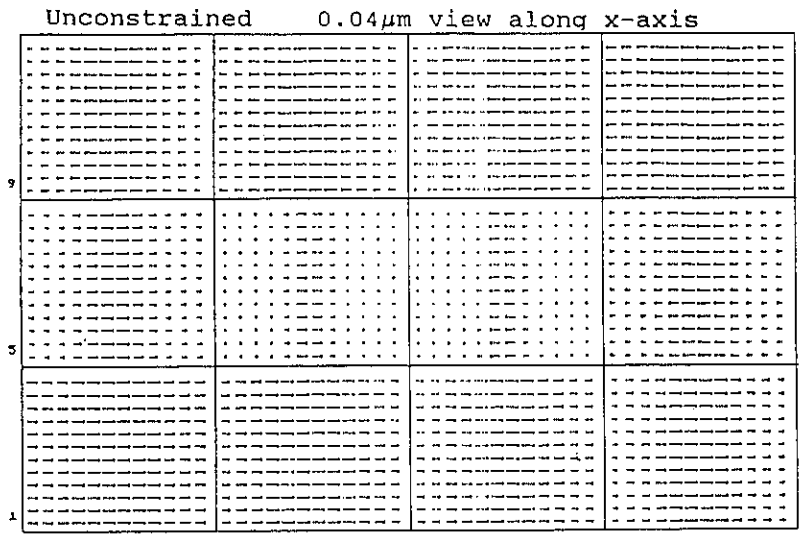

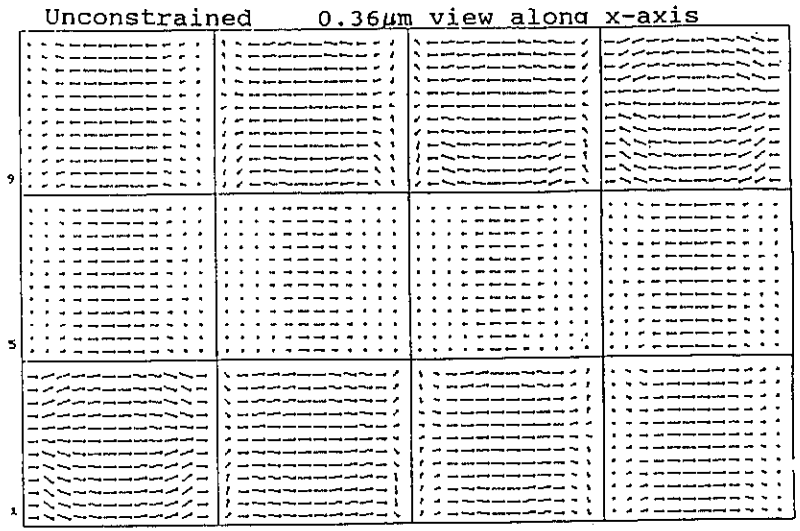

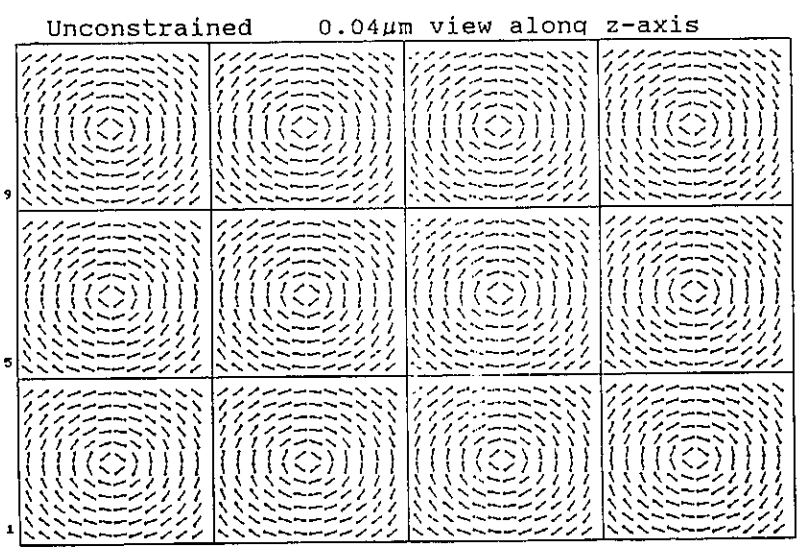

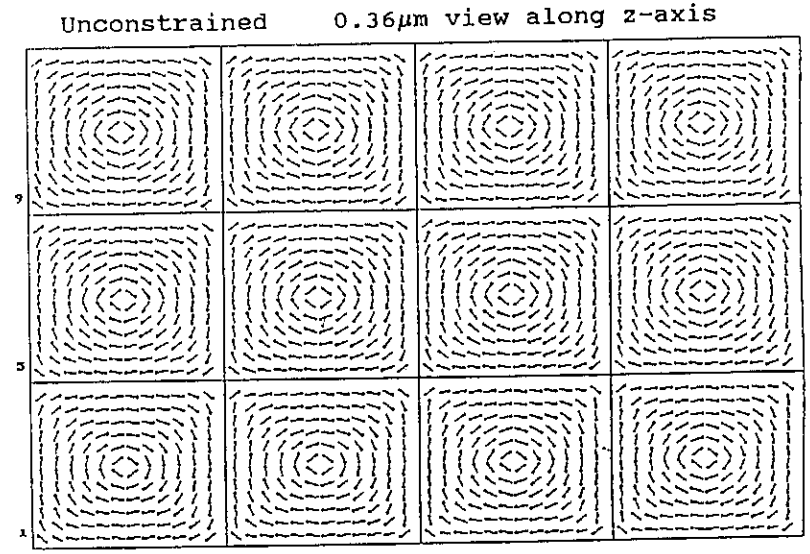

Appendix 2.3.

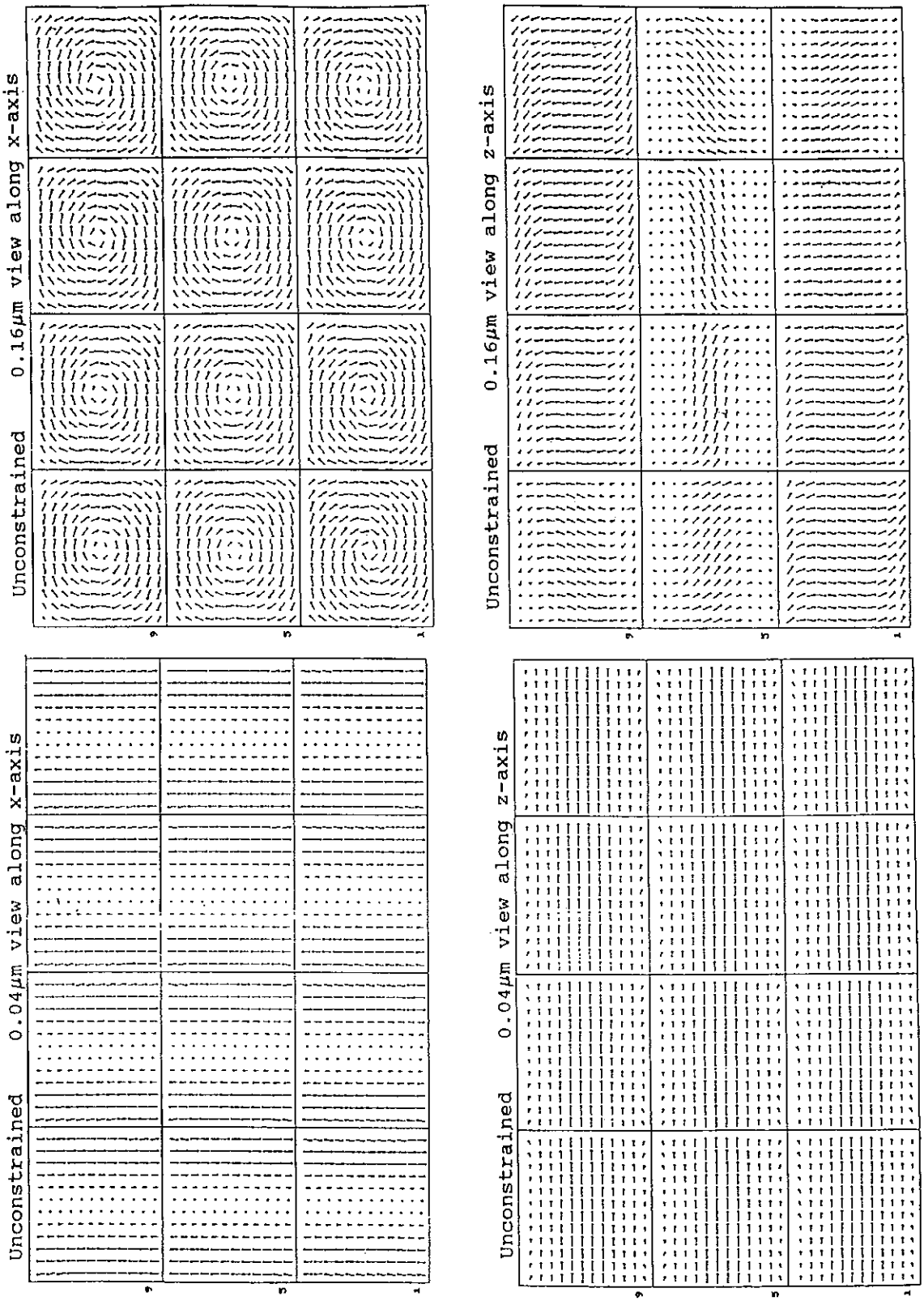
Initial state
Two-domain
Unconstrained 0.04μm view along x-axis
Unconstrained 0.04μm view along z-axis
Unconstrained 0.16μm view along x-axis
Unconstrained 0.16μm view along z-axis